105 (2026) 106904

Contents lists available at ScienceDirect

Poultry Science

journal homepage: www.elsevier.com/locate/psj

Full-Length Article

Integrated transcriptomics and metagenomics analyze the dynamic correlations between cecal mucosal tissue and cecal microbiota in Liangshan Yanying chickens during early postnatal development

Zengwen Huang [a], Jing Wang [a], Chaoyun Yang [a], Zengpeng Lv [b,*], Runjin Wang [c]

[a] Xichang University, Xichang, Sichuan, China
[b] China Agricultural University, Beijing, China
[c] Shannan Livestock and Poultry Breeding Center (Shannan Tibetan Chicken Industry Research Institute), Shannan, Tibet, China

ARTICLE INFO

Keywords:
Liangshan Yanying chicken
Cecal mucosal tissue
Cecal microbiota
Transcriptomics
Metagenomics

ABSTRACT

Liangshan Yanying chicken, a precious indigenous Chinese breed listed in the Catalog of Livestock and Poultry Genetic Resources in China, is an economic pillar in Liangshan Yi ethnic area and critical for poverty alleviation-to-rural revitalization transition. It has excellent phenotypic traits, high nutritional value, unique flavor, and strong adaptability to 380–4500 m altitudes. However, the co-evolutionary mechanism between its cecal mucosal tissue and gut microbiota (key to intestinal homeostasis and productivity) remains unclear. We systematically investigated their dynamic crosstalk in 1-, 14-, and 28-day-old chickens (n = 10/group) using transcriptomics, metagenomics, bioinformatics, and qPCR. Cecal length increased from 3.77 cm (1 d) to 8.98 cm (28 d), with higher growth rate at 14–28 d. We identified 67 DEGs (34 upregulated immune-related, 33 downregulated development-related) and 16 dynamically changed microbial taxa. Host-microbiota crosstalk was mediated by 52 shared KEGG pathways, with 10 core genes and 13 functional taxa maintaining homeostasis via PI3K-Akt pathway. This study first reveals a "gut microbial homeostasis" model for cecal dynamic homeostasis, providing insights for local poultry intestinal health and breeding.

Introduction

The intestinal tract of poultry serves as a permanent habitat for gut microbiota, encompassing diverse taxa including bacteria, archaea, viruses, and unicellular eukaryotes (Wickramasuriya et al., 2022). This microbiota primarily colonizes the gastrointestinal tract and is recognized as a critical "functional organ" in animals (Zhu et al., 2002). It not only positively regulates the intestinal mucosal immune system but also plays a core role in physiological processes such as food digestion and absorption, microbial protein synthesis, and vitamin biosynthesis (Kamada et al., 2013; Rodrigues, 2022). The composition, abundance, functions, and regulatory mechanisms of gut microbiota have become a research focus in recent years.

The chicken industry is an important pillar for ensuring China's meat, egg, and grain supply and increasing farmers' income. Gut microbiota exerts a key effect on the healthy growth and production performance of chickens. Among intestinal segments, the cecum has emerged as a core target for chicken gut microbiota research due to its unique characteristics: the highest microbial load (10^10–10^11 CFU/g), the longest digesta retention time (12–20 hours), and being the main fermentation site for short-chain fatty acids (SCFAs)(Yeoman et al., 2012). 16S rRNA sequencing results have shown that Lactobacillus dominates the duodenum, jejunum, and ileum of chickens, while the cecum is enriched with multiple taxa including Alistipes, Bacteroides, Butyricicoccus, Faecalibacterium, Lactobacillus, and Odoribacter, featuring high species richness and abundance(Xiao et al., 2017). Additionally, feed efficiency may regulate cecal microbial functions: chickens in the better feed efficiency (BFE) group exhibit significantly higher abundances of Lactobacillus and Akkermansia muciniphila in the cecum(Yan et al., 2017), further confirming the critical role of cecal microbiota in chicken growth, health, and physiological activities. Notably, two prerequisites must be met for microbiota to colonize and function in the intestine: recognition and acceptance of microbiota by the intestinal tract. This interaction is defined as a "gut microbial homeostasis" relationship in this study.

The interaction between chicken intestinal tissue and gut microbiota

* Corresponding author.
E-mail address: lvzengpeng310@cau.edu.cn (Z. Lv).

https://doi.org/10.1016/j.psj.2026.106904
Received 25 December 2025; Accepted 6 April 2026
Available online 9 April 2026

exhibits a "dynamic change–relative stability" pattern. Microbiota in different intestinal segments continuously evolve during early postnatal development (1–28 days of age), tend to mature by 28 days of age with peak diversity and metabolic capacity, and maintain stability from 28 days of age to adulthood (Zhang Yan, 2019;Huang et al., 2026).Therefore, 1–28-day-old chicks are commonly used as model subjects for chicken gut microbiota research.To establish terminological consistency across subsequent investigations, we formalize the definition of "gut microbial homeostasis" as the dynamic equilibrium governing the composition, abundance, and functional activities of niche-specified gut microbiota, modulated by animal species, individual differences, developmental phases, and intestinal compartments. This state is indispensable for maintaining intestinal physiological integrity and sustaining steady host-microbiota communication.However, the specific mechanism underlying the achievement of "homeostasis" between intestinal tissue and microbiota remains poorly explored.

To address this gap, the present study used Liangshan Yanying chickens as the research model. cecal mucosal tissues and contents were collected from three key growth stages (1, 14, and 28 days of age). Integrating transcriptomics and metagenomics techniques, we systematically deciphered the "gut microbial homeostasis" interaction between cecal mucosal tissue and microbiota at the molecular level (detailed workflow shown in Fig. 1). This study aims to reveal the interaction mechanism between chicken cecal mucosal tissue and gut microbiota, clarify the molecular basis of "homeostasis" formation, and provide theoretical support for related research fields.

Materials and methods

Ethics statement

All experiments adhered to the Animal Care and Use Guidelines of the Animal Care Committee of Xichang University (ACC-XU), China. The experimental protocol was approved by ACC-XU (Approval Number: xcc2022007). Every effort was made to minimize animal suffering and reduce the number of animals used.

Animals and sample collection

Fertilized eggs of Liangshan Yanying chickens were procured from Yuexi County Xinyi Ecological Breeding and Planting Professional Cooperative (Liangshan Prefecture, Sichuan, China), with 200 eggs prepared. All eggs were disinfected, weighed, numbered, and synchronously incubated in a "Fuhui" integrated incubator and brooder (Wuhan Fuhui Co., Ltd., China). Incubation parameters were set as follows: 37.8°C and 60% relative humidity (RH) on days 1–18, with egg turning every 2 hours; during days 19–21 (hatching period), temperature was adjusted to 37.2°C and RH raised to 70%. Candling was conducted on days 7, 11, and 19 to remove infertile eggs, dead sperm eggs, and dead embryo eggs respectively. The hatching rate of Liangshan Yanying chickens was 82.5% (165 chicks/200 eggs). Post-hatching, 120 healthy Liangshan Yanying chicken chicks were selected for rearing, with 4 replicate cages (30 chicks per cage) and extra chicks reserved as backups. Chicks were housed in standardized 2 m × 1 m cages under a cage-raising system, with each cage regarded as the experimental unit. Data were corrected at the cage level in subsequent statistical analyses to ensure reliability. Ad libitum feed and water were provided, following a staged feeding program: pre-starter diet for days 1–14 and starter diet for days 15–28. The diets, supplied by Kunming Bangyun Feed Co., Ltd., met the Chinese Feeding Standard for Chickens (NY/T 33-2004), with detailed nutritional compositions in Supplementary Table S1. Litter and feces were cleaned daily, and cages disinfected to maintain hygiene. No routine immunization was administered to ensure consistent experimental conditions. At 1, 14, and 28 days of age, 10 healthy chicks were

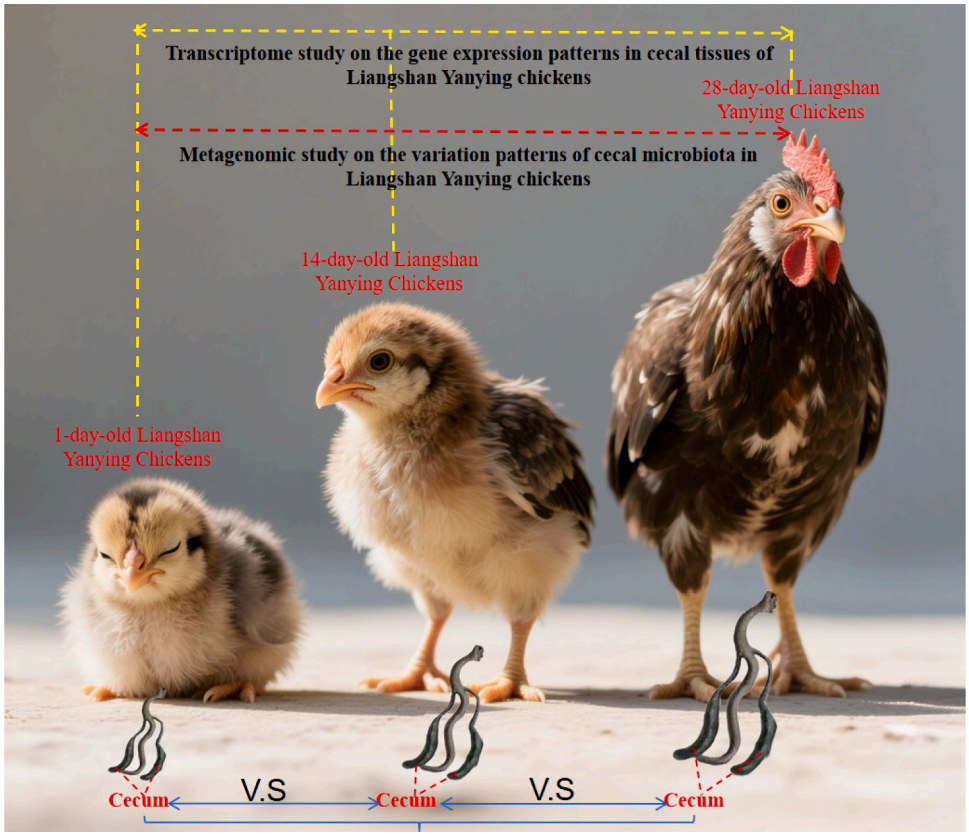

Fig. 1. Research framework diagram illustrating the interaction mechanism between cecal tissue gene expression patterns and microbial abundance changes in Liangshan Yanying chickens at different ages.

randomly selected. Chicks were euthanized by isoflurane inhalation anesthesia followed by jugular vein exsanguination. Under sterile conditions, cecal length was measured, and cecal mucosal tissue samples were collected into sterile cryopreservation tubes, quick-frozen in liquid nitrogen, transported to the laboratory, and stored at −80°C for subsequent analysis.

Determination of cecal length in Liangshan Yanying chickens at different ages

Ten Liangshan Yanying chickens were randomly selected at 1, 14, and 28 days of age, respectively. After euthanasia by jugular vein exsanguination, the abdominal cavity was dissected under sterile conditions to accurately locate the cecal mucosal tissue. Cecal length was measured using a vernier caliper. Each cecum was measured three times, and the average value was calculated to ensure data accuracy. Subsequently, cecal mucosal tissue samples were immediately frozen in liquid nitrogen and transferred to a −80°C ultra-low temperature refrigerator for subsequent molecular biological analysis. All operations were performed under strict sterile conditions to avoid potential contamination.

mRNA extraction, library construction, and sequencing of cecal mucosal tissues

Three chickens with significantly different cecal lengths were selected at each age (1, 14, and 28 days of age). Total RNA was extracted using the Trizol reagent (Invitrogen, Carlsbad, CA, USA), and the extracted products were stored at −80°C for subsequent library construction. After RNA purification, ribosomal RNA (rRNA) was removed, and eukaryotic mRNA with poly(A) tails was enriched using Oligo (dT) magnetic beads. The mRNA was fragmented by ultrasonication, and the fragmented mRNA was used as a template to synthesize the first strand of cDNA. Remaining RNA was degraded by RNaseH, followed by synthesis of the second strand of cDNA. Double-stranded cDNA underwent terminal repair, poly(A) tailing, and adaptor ligation. Fragments of approximately 200 bp were selected for PCR amplification. After purification of the amplified products, libraries were constructed and sequenced on the Illumina HiSeq2500 platform by Gene Denovo Biotechnology Co., Ltd. (Guangzhou, China).

Clean reads processing and quantification of gene abundance

To obtain high-quality sequencing reads, raw reads were subjected to quality control and purification. Specifically, reads containing adapter sequences, unknown nucleotides (N), low-quality bases ($q \leq 20$), and rRNA reads were removed. Clean reads (high-quality filtered reads) were aligned to the reference genome using the HISAT2 tool. FPKM (Fragments Per Kilobase of transcript per Million mapped reads) values were calculated using StringTie software to accurately quantify gene expression levels and variations. Differential expression analysis of RNA between groups was performed using DESeq2 software. DEGs were defined as those with a false discovery rate (FDR) < 0.05 and an absolute fold change ≥ 2 (corresponding to $|\log_2 FC| \geq 1$).

Bioinformatics analysis of DEGs

Principal Component Analysis (PCA) of samples from different ages (1, 14, and 28 days of age) was performed using the R package gmodels (http://www.rproject.org/). For DEGs between different ages, Gene Ontology (GO) annotation and enrichment analysis were conducted using clusterProfiler software, with $P < 0.05$ as the threshold to screen significantly enriched GO terms. Meanwhile, Kyoto Encyclopedia of Genes and Genomes (KEGG) pathway enrichment analysis of DEGs was performed to explore potential biological pathways.

DNA extraction, library construction, sequencing, and bioinformatics analysis of cecal microbiota

Three individuals exhibiting significant differences in cecal length were selected from each age group (1, 14, and 28 days old) for cecal content sampling. Genomic DNA was extracted from cecal contents using HiPure Bacterial DNA Kits (Magen, Guangzhou, China) following the manufacturer's protocol. DNA quality was assessed using Qubit and Nanodrop instruments (both from Thermo Fisher Scientific, Waltham, MA, USA). Qualified DNA was sonicated to approximately 350 bp fragments, which were then subjected to end repair, A-tailing, and adaptor ligation using the NEBNext® Ultra™ DNA Library Prep Kit for Illumina (NEB, Ipswich, MA, USA) according to the kit instructions. Fragments of 300–400 bp were enriched by PCR, and the amplified products were purified using the AMPure XP system (Beckman Coulter, Brea, CA, USA). Library size distribution was characterized with the 2100 Bioanalyzer (Agilent Technologies, Santa Clara, CA, USA), and library concentration was quantified by real-time PCR.

Metagenomic sequencing was performed on the Illumina Novaseq 6000 platform with 150 bp paired-end (PE) reads. De novo assembly of clean reads was conducted using MEGAHIT software. Open reading frames (ORFs) were predicted from assembled scaffolds via Prodigal and translated into amino acid sequences. A non-redundant gene set across all samples was constructed using CD-HIT, and gene abundance in each sample was quantified by Bowtie2. Representative sequences of the non-redundant gene set were aligned and annotated against the NR, COG, KEGG, and CAZy databases using DIAMOND and hmmscan (e-value $\leq$ 1e-5) to obtain species classification, KEGG functional annotations, and carbohydrate-active enzyme (CAZyme) annotations.

Data processing and statistical analysis

Transcriptomic data were statistically analyzed using WPS Office and SPSS 28.0 (IBM Corp., Armonk, NY, USA). Data are presented as mean ± standard deviation (SD). Differences between groups were assessed by one-way analysis of variance (one-way ANOVA), with $P < 0.05$ considered statistically significant. Graphs were generated using Origin 2022 (OriginLab Corporation, Northampton, MA, USA) and R4.0 software. Rapid multiple sequence alignment was performed using MUSCLE software.

For microbial α-diversity analysis, Chao1, Shannon, Simpson, and ACE indices were calculated using QIIME2 software. As microbiota data are non-normally distributed, the Kruskal-Wallis H test (a non-parametric test) was used instead of one-way ANOVA to test differences in α-diversity indices between groups (SPSS28.0, IBM Corp.), which is more suitable for non-normally distributed data. For differences in microbial composition at the phylum level, we first performed log10 transformation on the species abundance data to improve data normality before conducting statistical analysis. Significantly differential microbial taxa across different growth stages were screened using the Wilcoxon rank-sum test. Functional differences between groups (KEGG and Egg-NOG annotations) were inferred by PICRUSt software combined with alignment against the GreenGene database to calculate functional category abundances. Linear discriminant analysis effect size (LEfSe) was performed on the "BioinCloud" platform (https://bioincloud.tech/) to identify significantly differential taxa. Spearman correlation analysis between microbial taxa and functional pathways was conducted using the Psych package in R software, with $P < 0.05$ defined as statistically significant. A detailed description of the statistical method selection basis and data processing process for microbiota data is provided in the "Data Processing and Statistical Analysis" subsection.

Integrated analysis of cecal mucosal tissue transcriptomic and cecal microbiota metagenomic data

For the functional annotation and mechanistic deciphering of the

homeostatic interplay between cecal mucosal tissue and microbiota, we prioritized KEGG metabolic pathways demonstrating consistent co-enrichment signals in parallel transcriptomic and metagenomic analyses. All computational analyses, statistical modeling, and graphical outputs were generated using the R programming environment, Origin 2022b for data visualization, and WPS Office for document preparation.

Real-Time Quantitative PCR (qPCR) validation

Based on bioinformatics analysis results of DEGs, qPCR was performed to validate the expression levels of selected DEGs. Primers for DEGs were designed using Premier 5.0 software with reference to gene sequences in the NCBI database. Primer sequences are listed in Supplementary Table 2 and synthesized by Sangon Biotech (Shanghai, China). ArtiCanATM SYBR qPCR Mix (TSINGKE Biotech, Beijing, China) was used as the quantitative reagent, and reactions were carried out on the Applied Biosystems (ABI) ViiA 7 real-time PCR system (Thermo Fisher Scientific). Relative gene expression levels were calculated using the $2^{(-\triangle\triangle Ct)}$ method.

Results

Determination and analysis of cecal length in Liangshan Yanying chickens at different developmental stages

The descriptive statistics of cecum length at different ages and the results of multiple comparisons for significant differences among age groups are presented in Table 1. As shown in the table, the cecum length exhibited a continuous and extremely significant increasing trend with age. The mean values of cecum length at 1, 14, and 28 days of age were 3.76 ± 0.077 cm, 5.28 ± 0.079 cm, and 8.98 ± 0.368 cm, respectively, with corresponding coefficients of variation (CV) of 2.58%, 1.49%, and 4.10%. Among these, the 14-day-old individuals displayed the highest consistency in cecum development, while the 28-day-old individuals showed a slightly higher variation, although the overall level remained low.One-way analysis of variance (ANOVA) revealed an extremely significant overall difference among the three groups ($F = 182.300$, $df_{(between)} = 2$, $df_{(within)} = 27$, $P < 0.001$). Subsequent Tukey's HSD post-hoc tests demonstrated extremely significant differences in cecum length between any two age groups ($P < 0.001$). Specifically, the increase in cecum length from 14 to 28 days of age (69.90%) was significantly higher than that from 1 to 14 days of age (40.43%), indicating that 14–28 days of age represents the critical period for rapid cecum growth.

Table 1
Statistical Analysis of Cecum Length in Liangshan Yanying chicken at Different Developmental Stages.

Age (Days)	Mean ± Standard Deviation (cm)	Coefficient of Variation (CV, %)	Age Comparison and Significance of Differences	P-value
1Days	3.76±0.077	2.58	1Days vs 14Days	<0.001
14Days	5.28±0.079	1.49	1Days vs 28Days	<0.001
28Days	8.98±0.368	4.10	14Days vs 28Days	<0.001

Note: 1. Data are presented as Mean ± Standard Deviation (Mean ± SD), calculated by SPSS 26.0 software; 2. Coefficient of Variation (CV) reflects the degree of variation among individuals. A smaller CV indicates better consistency among individuals; 3. Comparisons among all age groups were subjected to Tukey's HSD multiple comparisons. A P-value < 0.001 was considered extremely significantly different (**); 4. The mean difference was calculated by subtracting the value of the later age from the earlier one. A negative value indicates that the cecum length at the later age was significantly longer than that at the earlier age; 5. Results of one-way analysis of variance (ANOVA): F = 182.300, df (between groups) = 2, df (within groups) = 27, P < 0.001.

Quality control of cecal mucosal tissue transcriptomic sequencing data

Transcriptomic sequencing was performed on cecal mucosal tissues from 1-, 14-, and 28-day-old chickens to explore dynamic changes in gene expression and differential expression between age groups (1 vs 14, 1 vs 28, 14 vs 28 days of age). After strict quality control, principal component analysis (PCA) showed significant intra-group clustering, indicating good reproducibility and high data similarity within groups, as well as clear inter-group separation (Fig. 2A). To visually present differences in gene abundance among groups, violin plots were used to display data distribution and gene expression dispersion (Fig. 2B). Results showed that the median, interquartile range, and gene expression distribution of samples within each group were relatively consistent, further verifying the high reproducibility of parallel samples. Sample correlation analysis yielded consistent results, confirming that the transcriptomic data were of high quality and suitable for subsequent in-depth analysis.

Gene annotation and statistical analysis of cecal mucosal tissue transcriptomic sequencing

After strict pre-sequencing quality control, sequencing data were aligned to the Gallus gallus (chicken) reference genome, and FPKM (Fragments Per Kilobase of transcript per Million mapped reads) values were calculated using StringTie software. Using FPKM > 0 as the screening criterion, 16,147, 16,195, and 16,298 gene IDs were annotated in cecal mucosal tissues at 1, 14, and 28 days of age, respectively. After data filtering and gene annotation, 13,623, 13,611, and 13,633 expressed genes were obtained for the three age groups. KEGG annotation results showed that 5,582, 5,590, and 5,598 genes were annotated to KEGG pathways at 1, 14, and 28 days of age, respectively (Fig. 3A). For GO (Gene Ontology) annotation, which includes three categories [Cellular Component (CC), Molecular Function (MF), Biological Process (BP)], the numbers of annotated genes were as follows: 4,689 (CC), 5,066 (MF), and 4,974 (BP) at 1 day of age; 4,685 (CC), 5,066 (MF), and 4,976 (BP) at 14 days of age; and 4,687 (CC), 5,065 (MF), and 4,974 (BP) at 28 days of age (Fig. 3B).

Comparative analysis of DEGs in cecal mucosal tissues at different developmental stages

To explore the characteristics of DEGs in cecal mucosal tissues of Liangshan Yanying chickens at 1, 14, and 28 days of age, DEGs were screened using the criteria of $|\log_2 FC| > 1$ and FDR < 0.05. Results showed that a total of 1,286 DEGs were identified between the 1-day and 14-day age groups (750 upregulated and 536 downregulated in the 1-day age group); 893 DEGs were found between the 14-day and 28-day age groups (537 upregulated and 356 downregulated in the 14-day age group); and the largest number of DEGs (1,844) was detected between the 1-day and 28-day age groups (1,157 upregulated and 687 downregulated in the 1-day age group) (Fig. 4). After joint annotation by KEGG and GO, valid DEGs were obtained as follows: 449 (272 upregulated, 177 downregulated) in the 1 vs 14-day group; 297 (165 upregulated, 132 downregulated) in the 14 vs 28-day group; and 672 (416 upregulated, 256 downregulated) in the 1 vs 28-day group. Additionally, expression trend clustering analysis of DEGs across the three groups revealed 34 persistently upregulated genes and 33 persistently downregulated genes in cecal mucosal tissues from 1 to 28 days of age (Supplementary Table 3).

qPCR validation of DEGs and expression pattern analysis in cecal mucosal tissues

To verify the accuracy of transcriptomic sequencing data, qPCR was performed on four significantly DEGs —BLVRA, IRF4, ALPI, and CLCA1—screened from cecal mucosal tissues of 1-, 14-, and 28-day-old

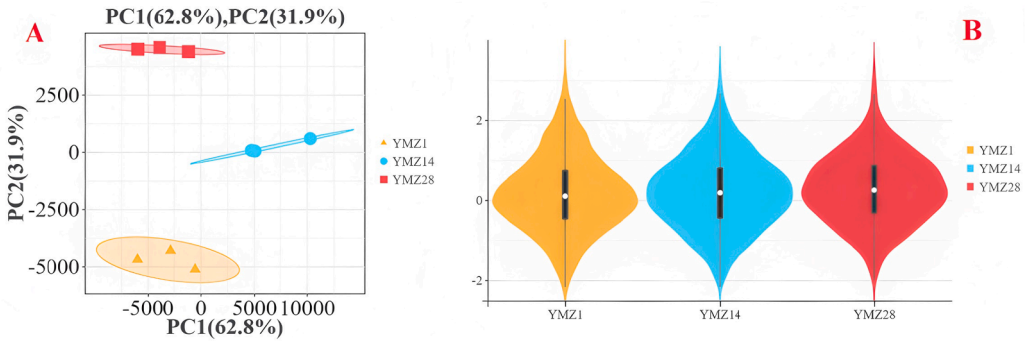

Fig. 2. Principal component analysis (PCA) and violin plots of transcriptomic data from the cecal tissues of Liangshan Yanying chickens at 1, 14, and 28 days of age.
Note: YMZ1 = 1-day-old cecal tissue; YMZ14 = 14-day-old cecal tissue; YMZ28 = 28-day-old cecal tissue of Liangshan Yanying chickens.

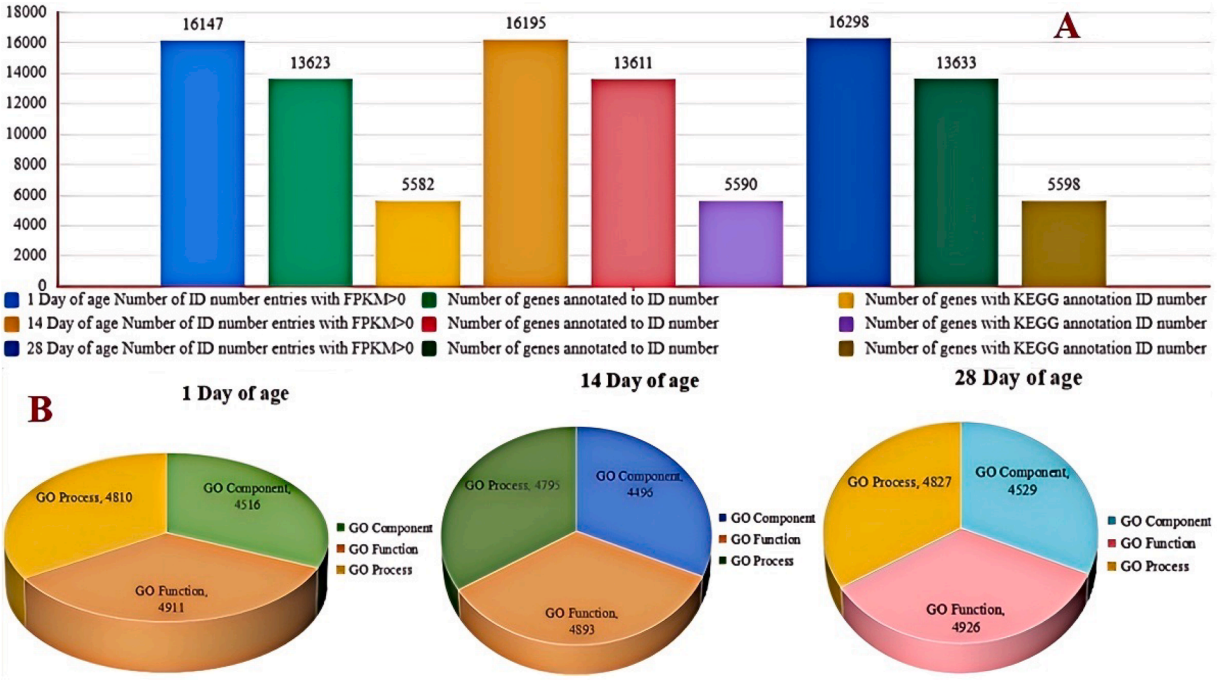

Fig. 3. Statistical analysis of transcriptomic data from the cecal tissues of 1-, 14-, and 28-day-old Liangshan Yanying chickens.
Note: Consistent with the annotation in Fig. 2.

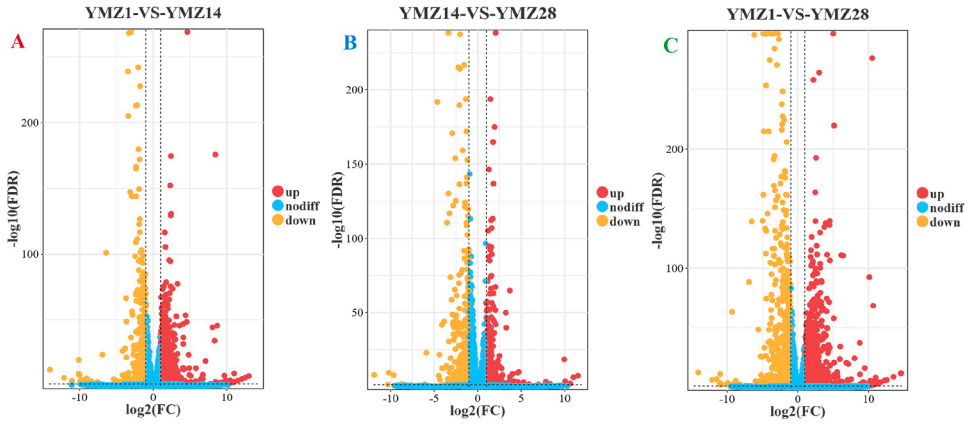

Fig. 4. Volcano plot analysis of differentially expressed genes (DEGs) in Liangshan Yanying chickens at different ages.

Liangshan Yanying chickens. Results showed that the expression trends of these genes across different ages were highly consistent with RNA-seq data (Fig. 5), confirming the reliability of the transcriptomic results. Further analysis of their expression patterns revealed that the expression

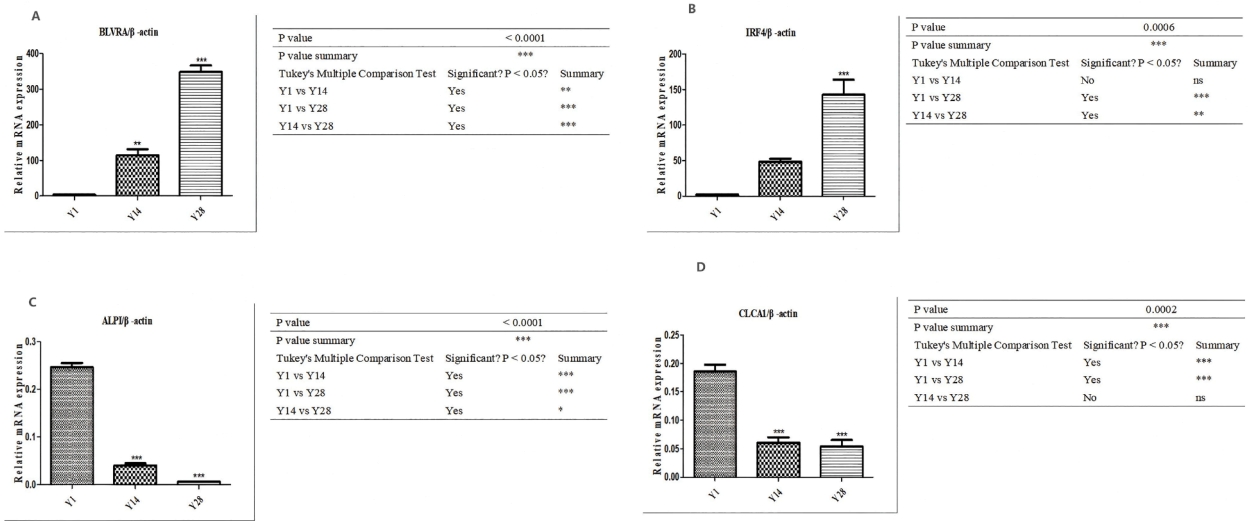

Fig. 5. Quantitative PCR (qPCR) validation of transcriptomic results for the cecal tissues of Liangshan Yanying chickens.

levels of cecum development-related genes (CLCA1, ALPI) showed a phased decrease with increasing age, while those of immune-related genes (IRF4, BLVRA) gradually increased. These findings suggest that the disease resistance potential of Liangshan Yanying chickens continuously enhances with age.

Quality control and overview of cecal microbiota metagenomic sequencing data

Metagenomic sequencing was performed on 9 qualified cecal content samples using the Illumina Novaseq 6000 platform, generating a total of 613,406,086 raw reads. After quality control filtering and host DNA removal, 612,392,454 clean reads and 608,335,364 effective reads were obtained. Integrated data were assembled into 1,443,611 contigs (length $>$ 500 bp). Statistical analysis showed: 963,482 contigs with an average gene length of 1,042 bp in 1-day-old samples; 1,330,156 contigs with an average length of 1,073 bp in 14-day-old samples; and 1,281,260 contigs with an average length of 1,085 bp in 28-day-old samples. A total of 1,048,575 unigenes were predicted from these contigs, including 136,812, 207,783, and 185,483 unigenes identified in 1-, 14-, and 28-day-old samples, respectively (Table 2). Visualization analysis of unigenes showed 31,347 shared unigenes among the three age groups, with 76,218, 69,941, and 63,490 age-specific unigenes in 1-, 14-, and 28-day-old samples, respectively (Fig. 6).

Functional annotation analysis of cecal microbiota unigenes at different ages

Unigenes identified from cecal contents of 1-, 14-, and 28-day-old chickens were dereplicated using DIAMOND software (e-value $\leq$ 1e-5) to obtain a non-redundant gene set. This set was then annotated by alignment against seven databases: NR (Non-Redundant Protein

Table 2
Assembly and sequencing information statistics of all samples.

Sample	Raw Reads (bp)	Clean reads(%)	Effective reads (bp)	Contigs Numbe r (>500 bp)	N50	Gene Number	Total Length Gene Length	Average Length	GC%	Unigene
YMN1-1	62536264	62426342 (99.82%)	62235946	91713	4767	240230	246859263	1027	54.96%	136812
YMN1-2	69863188	69699338 (99.77%)	68084368	107787	6935	373433	401105025	1074	54.65%	
YMN1-3	66090490	65993486 (99.85%)	65983396	116357	5398	349819	356350758	1018	55.76%	
YMN14-1	66347470	66251032 (99.85%)	66236990	189681	3522	479490	496770960	1036	55.62%	207783
YMN14-2	65105170	65021086 (99.87%)	64896644	192918	3639	451502	490227993	1085	55.55%	
YMN14-3	67407364	67294858 (99.83%)	66705762	179713	4154	399164	441131019	1105	55.96%	
YMN28-1	83869360	83724230 (99.83%)	83669786	219340	3059	441656	481736214	1090	54.85%	185483
YMN28-2	66664660	66550326 (99.83%)	65109012	158579	3596	332615	380539248	1144	55.02%	
YMN28-3	65522120	65431756 (99.86%)	65413460	187523	4238	506989	528581850	1042	55.20%	

Note:YMN1: Refers to the contents of the cecum of 1-day-old Liangshan Yanying Chicken; YMN14: Refers to the cecal contents of 14-day-old Liangshan Yanying Chicken; YMN28: Refers to the contents of the cecum of 28 day old Liangshan Yanying Chicken;Raw Reads:Obtain raw data after sequencing; Effect Reads: valid data obtained after quality control and used for subsequent analysis; Contigs Number: the number of contigs obtained after assembling effective reads; N50: sort all Contigs according to their length, and then add them from long to short, and the length value of Contigs when the added value reaches 50% of the total length of Contigs; Gene Number: the number of genes in this sample in the non-redundant gene set; Total Length Gene Length: the total length of all genes in this sample;Average Length:The ratio of total gene length to the number of genes; GC%: The percentage of GC bases of genes in the sample to the total number of bases;Unigene:Unigene is the abbreviation for Universal Gene, which means a widely used gene database. It is formed by collecting and organizing the same locus (Locus) on a computer to form a non redundant gene database.

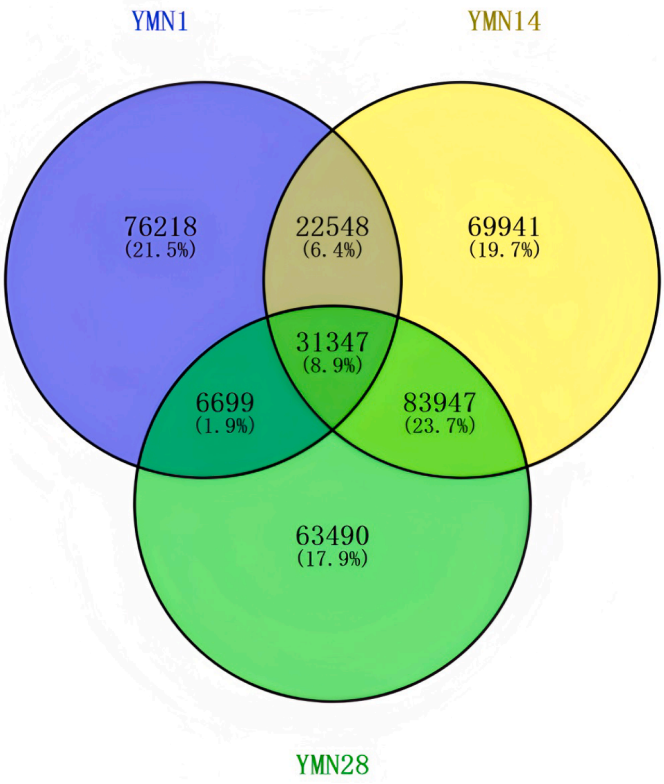

Fig. 6. Quality control analysis of microbial metagenomic sequencing data from the ceca of Liangshan Yanying chickens.

Sequence Database), KEGG (Kyoto Encyclopedia of Genes and Genomes), eggNOG (Evolutionary Genealogy of Genes: Non-supervised Orthologous Groups), CAZy (Carbohydrate-Active Enzymes Database), VFDB (Virulence Factors of Pathogenic Bacteria Database), PHI (Pathogen-Host Interactions Database), and CARD (Comprehensive Antibiotic Resistance Database). Functional differences between groups were analyzed based on gene abundance data. Annotation results (Supplementary Table 4) showed: 965,030 genes annotated to NR, 859,869 to KEGG, 868,337 to eggNOG, 187,539 to CAZy, 117,459 to VFDB, 175,512 to PHI, and 50,377 to CARD. Statistical analysis indicated that unigenes were mainly enriched in the NR, KEGG, and eggNOG databases, and subsequent in-depth analyses were based on annotations from these three databases.

Species annotation and community composition characteristics of cecal microbiota

Species annotation of unigenes from cecal contents was performed by alignment against the NR database using DIAMOND software (e-value $\leq$ 1e-5). Results showed that unigenes were annotated to six kingdoms: Archaea, Bacteria, Eukaryota, Fungi, Metazoa, and Viruses. Among these, Bacteria had the highest relative abundance, accounting for an average of 99.9%. Further annotation revealed 121 phyla, 180 classes, 291 orders, 498 families, 1295 genera, and 4579 species. Comparative analysis of microbial communities across ages showed dynamic changes in the composition and quantity of cecal microbiota from 1 to 28 days of age: 1768, 2461, and 2464 microbial species were detected at 1, 14, and 28 days of age, with 174, 267, and 337 age-specific species, respectively. A total of 1411 species were shared among the three age groups (Fig. 7), indicating significant differences in microbial composition patterns across different developmental stages.

KEGG functional annotation analysis of cecal microbiota at different ages

Unigenes from cecal contents of 1-, 14-, and 28-day-old chickens were annotated by alignment against the KEGG database using DIAMOND software (e-value $\leq$ 1e-5), with 279,891 unigenes successfully annotated. These annotations were distributed across 6 main categories (Metabolism, Environmental Information Processing, Cellular Processes, Genetic Information Processing, Human Diseases, Organismal Systems),

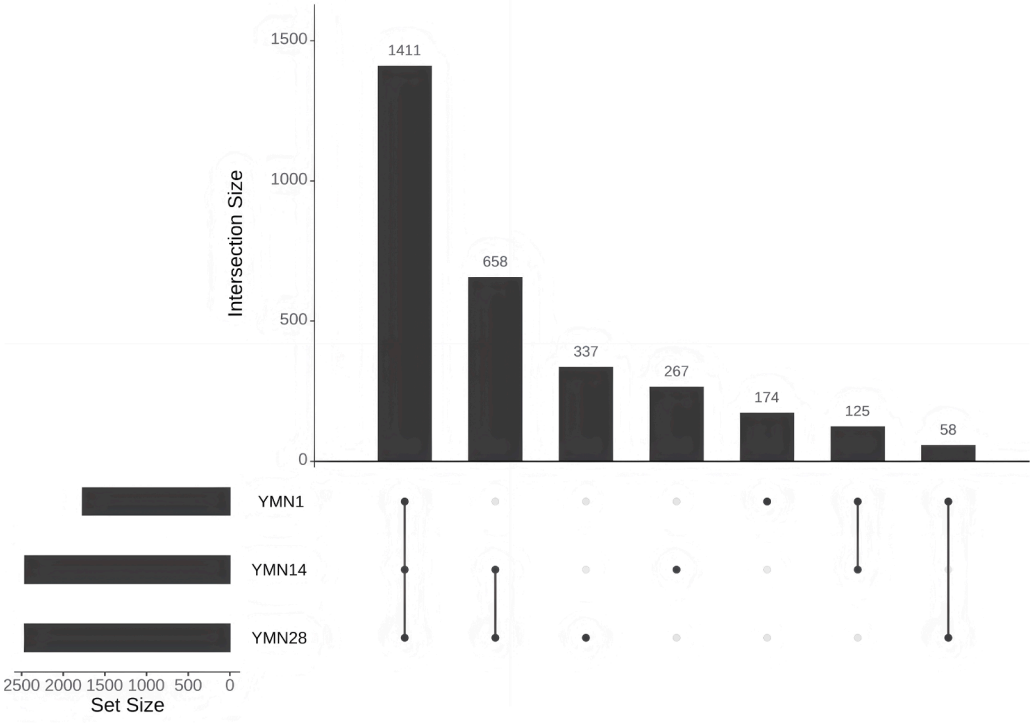

Fig. 7. Comparative analysis of species annotations for the cecal microbial community composition in Liangshan Yanying chickens at different ages.

42 subcategories, and 303 metabolic pathways. The top 5 pathways with the highest gene enrichment were: Metabolic pathways (158,270 genes), Biosynthesis of secondary metabolites (70,036 genes), Microbial metabolism in diverse environments (40,359 genes), Biosynthesis of amino acids (33,019 genes), and ABC transporters (24,150 genes). Bar charts intuitively show the distribution of gene counts across different classification levels (Fig. 8), while functional abundance analysis of sample genes reveals inter-group distribution patterns and characterizes KEGG functional abundance at each level (Fig. 9).

α and β diversity analysis of cecal microbiota in Liangshan Yanying chickens at different ages

To evaluate the richness and diversity of cecal microbial communities in Liangshan Yanying chickens at 1, 14, and 28 days of age, multiple statistical indices were used for α-diversity analysis. The Chao and Ace indices reflect species richness without weighting species abundance or individual counts. The Shannon and Simpson indices measure community diversity, influenced by both species richness and evenness—higher evenness indicates greater diversity.

Kruskal-Wallis rank-sum test showed no significant differences in Chao and Ace indices among the three age groups ($P = 0.118$), but significant differences were observed in diversity indices. The Simpson index ($P = 0.05091$) followed the order: 1-day-old (0.8643 ± 0.1129) < 14-day-old (0.9775 ± 0.0031) > 28-day-old (0.9658 ± 0.0064). The Shannon index ($P = 0.03899$) showed a similar trend: 1-day-old (4.9321 ± 1.6881) < 14-day-old (7.2499 ± 0.1234) > 28-day-old (6.8143 ± 0.2409), indicating the highest microbial diversity at 14 days of age. Overall, with increasing age, cecal microbial species became more abundant, abundance indices gradually increased, and sample homogeneity improved.

β-diversity analysis revealed significant differences in cecal microbial structure among the three age groups. A unigene-based sample model was constructed using the UniFrac distance matrix. Principal Coordinate Analysis (PCoA) at the phylum level showed clear separation of sample distribution areas, indicating significant differences in microbial composition at the phylum level (Fig. 10A). PERMANOVA analysis at the class level yielded $R^2 = 0.7101$ and $P = 0.005$, confirming statistically significant differences in microbial communities at the class level (Fig. 10B). PERMANOVA analysis at the order level showed $R = 0.572$ and $P = 0.004$, suggesting that inter-group differences were significantly greater than intra-group differences (Fig. 10C). Visualization of the Bray-Curtis distance index at the species level showed distinct clustering of the three sample groups, indicating significant differences in microbial composition at the species level (Fig. 10D). Collectively, cecal microbial communities of Liangshan Yanying chickens differed significantly across multiple taxonomic levels at 1, 14, and 28 days of age, which may be associated with age-related adaptive changes in gut microbiota.

Screening and identification of specifically colonized cecal microbial communities at different ages

Focusing on the abundance characteristics of cecal microbiota in Liangshan Yanying chickens at 1, 14, and 28 days of age, Linear Discriminant Analysis Effect Size (LefSe) was used to identify significantly differential dominant communities/species across developmental stages. This method combines hypothesis testing and significance assessment of abundance differences, based on taxonomic composition and grouping conditions, to screen specifically colonized microorganisms in the cecum. Results showed distinct differences in specifically colonized microorganisms among different ages: 52 species at 1 day, 37 species at 14 days, and 46 species at 28 days (Fig. 11A).KEGG database functional annotation indicated that the specific microorganisms in the three age groups corresponded to 25, 3, and 39 specific functional categories, respectively. Core functions included transport and metabolism of carbohydrates and amino acids, replication/recombination/repair, translation, ribosomal structure and biogenesis, and transcription. Additional functions involved amino acid metabolism, energy metabolism, lipid transport, nucleotide metabolism and transport, and signal transduction (Fig. 11B). All results are presented as a phylogenetic tree, intuitively showing significant differences in species composition and functional characteristics of cecal microbiota across different ages.

Integrated analysis of cecal transcriptomic and microbial metagenomic data across different growth stages

Transcriptomic data of cecal mucosal tissues and metagenomic data of cecal microbiota from 1 to 28-day-old Liangshan Yanying chickens were integrated, combined with Spearman correlation analysis (Fig. 12) and visualization for systematic investigation. Transcriptomic analysis identified 34 persistently upregulated genes and 33 persistently downregulated genes in cecal mucosal tissues from 1 to 28 days of age. Metagenomic analysis showed 14 persistently increased and 2 persistently decreased microbial species during the same period.

After data normalization, K_ID annotation and Pathway analysis were performed on 67 persistently changing genes (1 gene, P2RY10, was not successfully annotated), resulting in enrichment of 153 pathways. Among these, ko04974 had the highest number of enriched genes (11). Annotation of 16 persistently changing microbial species using Unigene_ID yielded 3793 unigenes (Pseudoflavonifractor capillosus had the highest annotation count: 3065). A total of 1653 unigenes from 13 microbial species were successfully annotated to KEGG orthologs (ko), enriching 214 pathways. Further integrated analysis revealed 52 shared pathways enriched by both transcriptomic and metagenomic data, with ko01100 (Metabolic pathways) containing the most entries (involving 8 genes and 13 microbial species). According to KEGG_A_class classification: 2 pathways in Cellular Processes (2 genes, 4 microbial taxa), 6 pathways in Environmental Information Processing (9 genes, 8 microbial taxa), 20 pathways in Human Diseases (17 genes, 4 microbial taxa), 11 pathways in Metabolism (8 genes, 13 microbial taxa), and 13 pathways in Organismal Systems (16 genes, 4 microbial taxa). All data were classified and visualized at three levels: KEGG_A_class, KEGG_B_class, and Pathway (Fig. 13).

Molecular network interaction analysis between DEGs in cecal mucosal tissues and gut microbiota

Ten significantly DEGs in cecal mucosal tissues and 13 cecal microbial species enriched in shared pathways were selected for molecular network interaction analysis. Results showed that these genes and microorganisms were jointly enriched in 12 pathways of KEGG_A_class, covering three categories: Environmental Information Processing, Metabolism, and Organismal Systems. Among these, Metabolic pathways contained the largest total number of enriched genes and microorganisms (15), followed by Porphyrin and chlorophyll metabolism (7). Thiamine metabolism, PI3K-Akt signaling pathway, and Pancreatic secretion each contained 4 enriched entries. Further interaction analysis confirmed significant interactions between the 10 DEGs and 13 microbial species, with the molecular network interaction characteristics shown in Fig. 14.

Discussion

As a core digestive organ, the intestine is critical for nutrient absorption and determines chicken production performance (Latek et al., 2022). Previous studies have confirmed strain (Chen Lianyi et al., 2014), diet (Cao Xiangyang, 2011), and rearing environment (Fang Li et al., 2018)as key regulators of intestinal development, e.g., Guan et al.(Guan Lihui et al., 2017)and Hu(Hu Lingling, 2013, 2013)reported dietary metabolizable energy affects intestinal morphology in different chicken breeds. This study focused on 1–28-day-old Liangshan Yanying

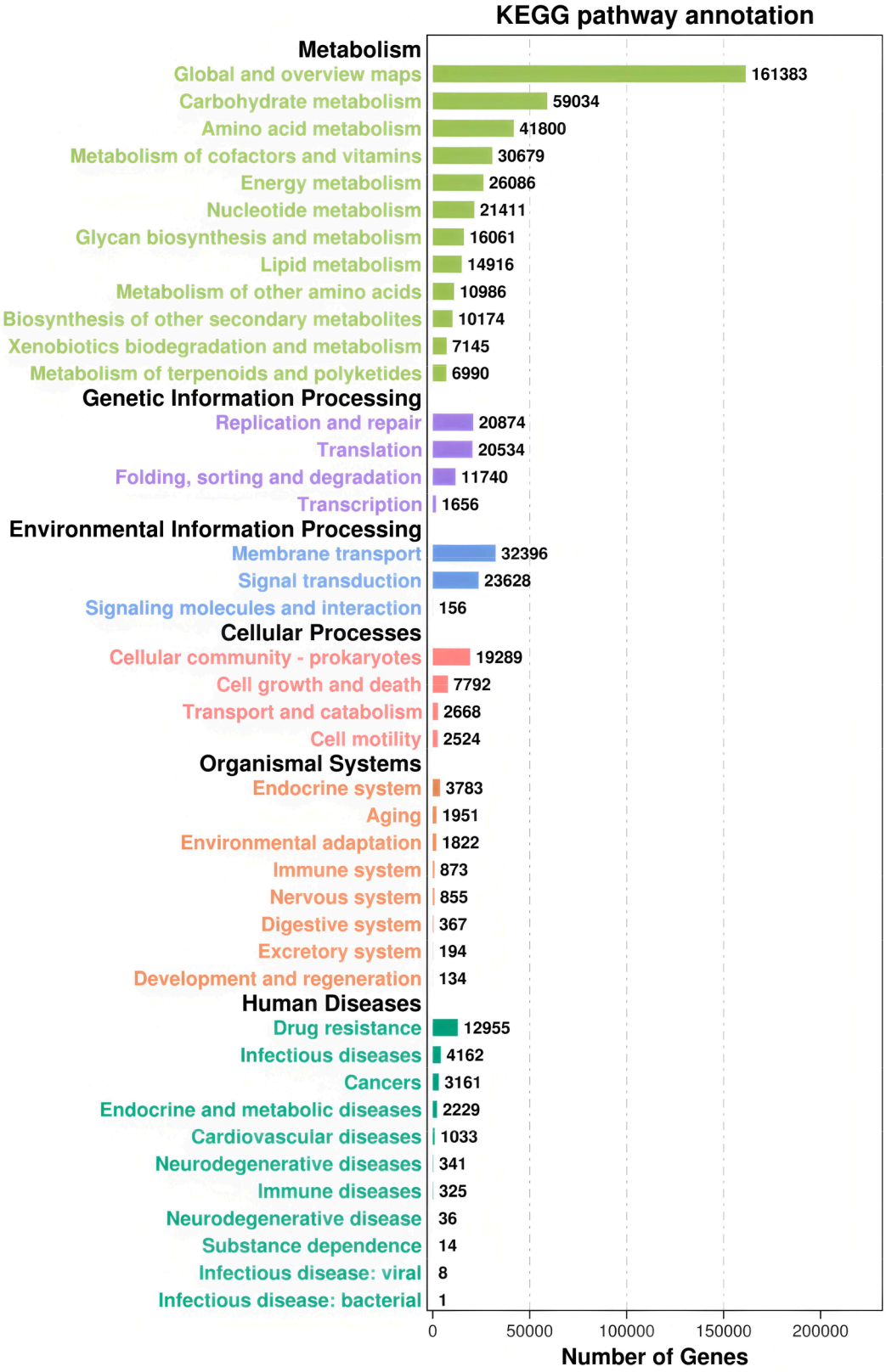

Fig. 8. Kyoto Encyclopedia of Genes and Genomes (KEGG) functional annotation analysis of cecal microbial communities in Liangshan Yanying chickens at different ages.

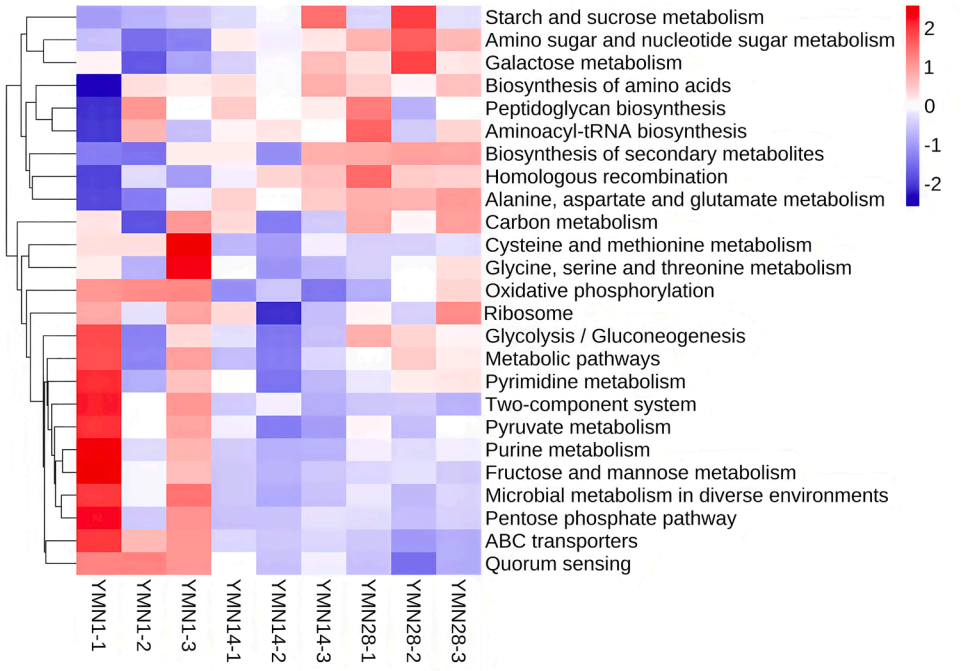

Fig. 9. Heatmap analysis of annotated pathways in the cecal microbial communities of Liangshan Yanying chickens at different ages.

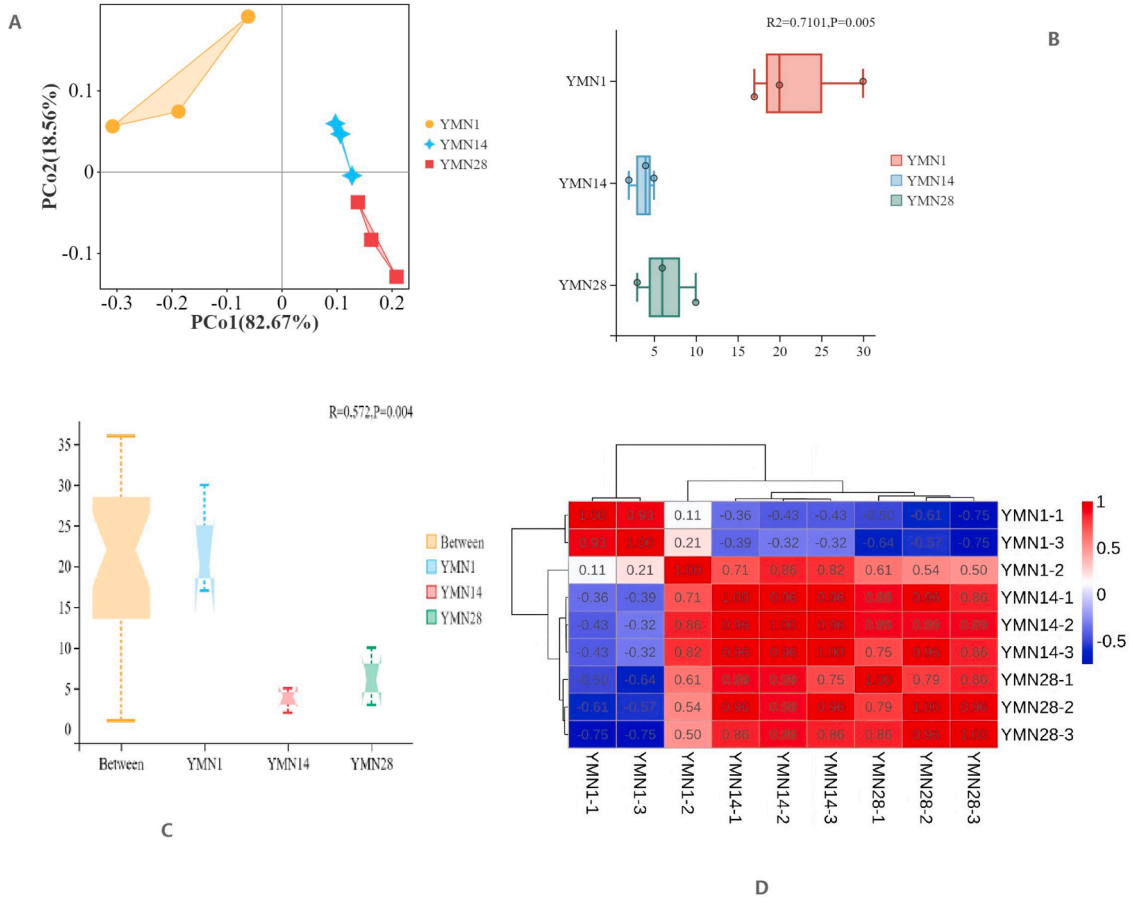

Fig. 10. Beta diversity analysis of the cecal microbiota in Liangshan Yanying chickens at different days of age.

chickens, finding a significant positive correlation between cecal length and age, with distinct stage-specific growth rates (1–14 vs. 14–28 days). Notably, its higher cecal growth rate at 14–28 days is consistent with local breeds (e.g., Gushi chickens) but differs from fast-growing broilers (e.g., Cobb broilers, rapid growth at 1–14 days), possibly related to genetic characteristics of slow-growing local breeds. This study

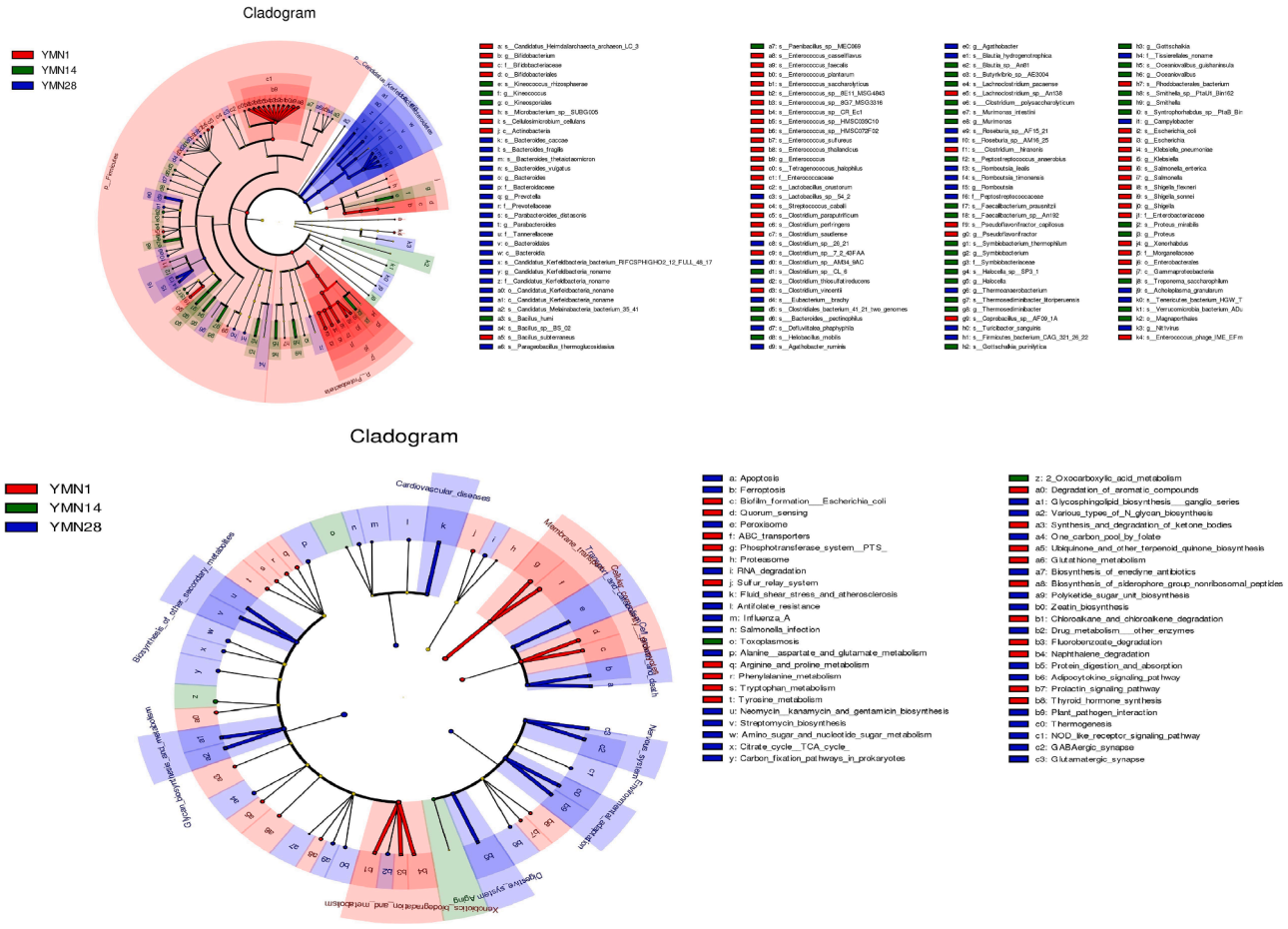

Fig. 11. Screening and characterization of age-specific colonizing microbial communities in the ceca of Liangshan Yanying chickens.

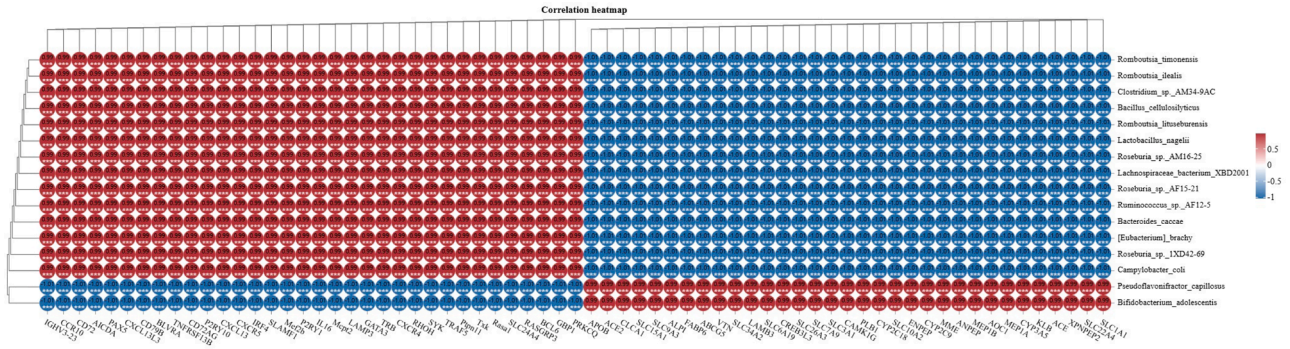

Fig. 12. Integrated analysis of cecal tissue transcriptomics and cecal microbial metagenomics data from Liangshan Yanying chickens at different growth stages.

supplements basic data for poultry intestinal development research and provides a basis for breed-specific nutritional management.

Environmental information processing pathways mediate the cecal regulatory responses to external stimuli, while metabolic pathways govern intestinal energy metabolism and substance transport. The angiotensin-converting enzyme 2 (ACE2) gene facilitates intestinal nutrient and amino acid transport by dilating intestinal blood vessels (Perlot and Penninger, 2013), but this study demonstrated a age-dependent decrease in its expression, highlighting the need for further investigation into its regulatory mechanisms in chicken digestive tract function. Quantitative real-time polymerase chain reaction (qPCR) validation of four randomly selected DEGs confirmed the accuracy of the transcriptomic data. The synergistic interaction between gut microbiota and the host is critical for maintaining chicken health and production performance (Stanley et al., 2014), as it promotes nutrient absorption (Rodríguez et al., 2015) and regulates immune function (Young et al., 2007; Brisbin et al., 2008). Analysis of cecal microbiota in 1–28-day-old Liangshan Yanying chickens revealed 16 core microbial species with dynamic abundance changes (14 showing an upward trend), including short-chain fatty acid (SCFA)-producing bacteria, cellulose/polysaccharide-degrading bacteria, butyrate-producing bacteria, lactic acid-fermenting bacteria, and potential pathogenic bacteria, all of which play pivotal roles in regulating feed utilization, intestinal health, and microecological balance. Dynamic changes in Romboutsia sp.(Gerritsen et al., 2017; Yin et al., 2023) and Ruminococcus sp. AF12-5 (La Reau and Suen, 2018; Saad et al., 2021; Wang et al., 2024)further

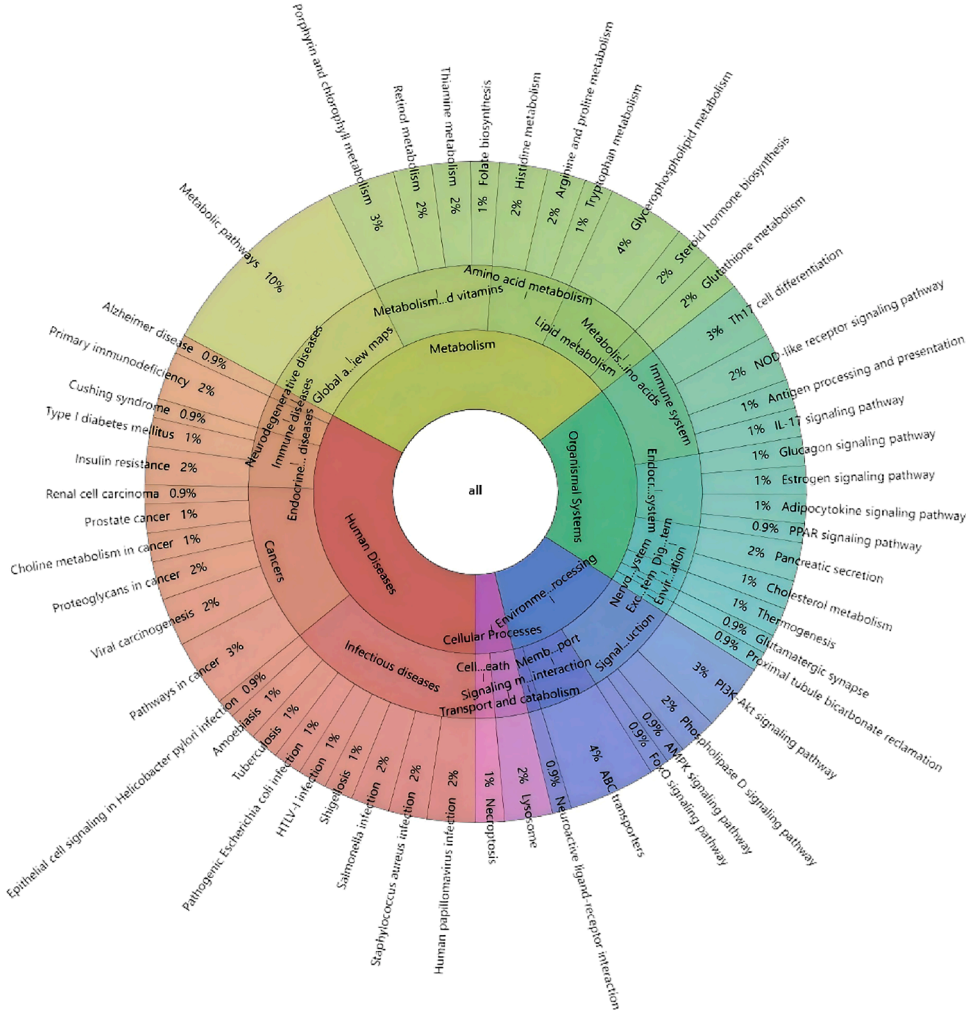

Fig. 13. Pathway-integrated gene analysis of cecal tissue changes and cecal microbial annotations in Liangshan Yanying chickens at various days of age.

support the involvement of functional microbiota in chicken growth and health maintenance. The enrichment of SCFA-producing and cellulose-degrading bacteria is consistent with that of other forage-adapted poultry, while the unique abundance of Lactobacillus nagelii may be associated with the local feeding environment and genetic background of Liangshan Yanying chickens. Additionally, the conserved PI3K-Akt signaling pathway confirms the universality of this regulatory pathway in poultry intestinal host-microbiota interactions.

Collectively, these findings not only deepen our systematic understanding of the morphological development, gene expression patterns, and microbial community succession in the cecum of Liangshan Yanying chickens but also provide a novel perspective for deciphering the regulatory mechanisms underlying the interactions between host genes and the gut microbiota. Importantly, this study carries significant scientific value and practical implications for guiding the healthy and efficient breeding of poultry, laying a solid foundation for the subsequent optimization of breeding strategies and the improvement of poultry production performance.

To further expand the scope of this research and address the remaining questions, we propose the following follow-up research directions: (1) Conducting in vitro cell culture experiments to verify the regulatory effects of core genes (e.g., BLVRA, IRF4) on the function of intestinal epithelial cells and the regulation of immune responses; (2) Performing germ-free chicken colonization experiments to validate the causal role of core microbial taxa (e.g., Bacteroides caccae, Lactobacillus nagelii) in the development and homeostasis maintenance of cecal tissue; (3) Carrying out gene knockout/overexpression experiments combined with microbial intervention strategies to clarify the molecular regulatory network of the "gut microbial homeostasis" model, thereby revealing the intrinsic link between host genetic factors and gut microbial colonization.

Conclusion

By integrating transcriptomics and metagenomics, this study systematically revealed the mechanism by which the cecal mucosal tissue and microbiota of Liangshan Yanying chickens co-evolve through a "gut microbial homeostasis" model to maintain dynamic homeostasis during early development. Results showed that cecal length exhibited significant stage-specific growth, accompanied by programmed changes in tissue gene expression—characterized by the persistent upregulation of immune-related genes (e.g., IRF4, BLVRA) and persistent downregulation of development-related genes. Meanwhile, the abundance of 16 core functional microbial taxa displayed dynamic changes, and these microbes were co-enriched with host genes in 52 KEGG pathways. Molecular interaction network analysis demonstrated that the host and microbiota engage in precise crosstalk primarily through signaling pathways such as PI3K-Akt, collectively maintaining cecal microenvironment homeostasis. This study provides a crucial theoretical basis for understanding the intestinal health mechanisms of local chicken breeds and formulating precise breeding strategies.

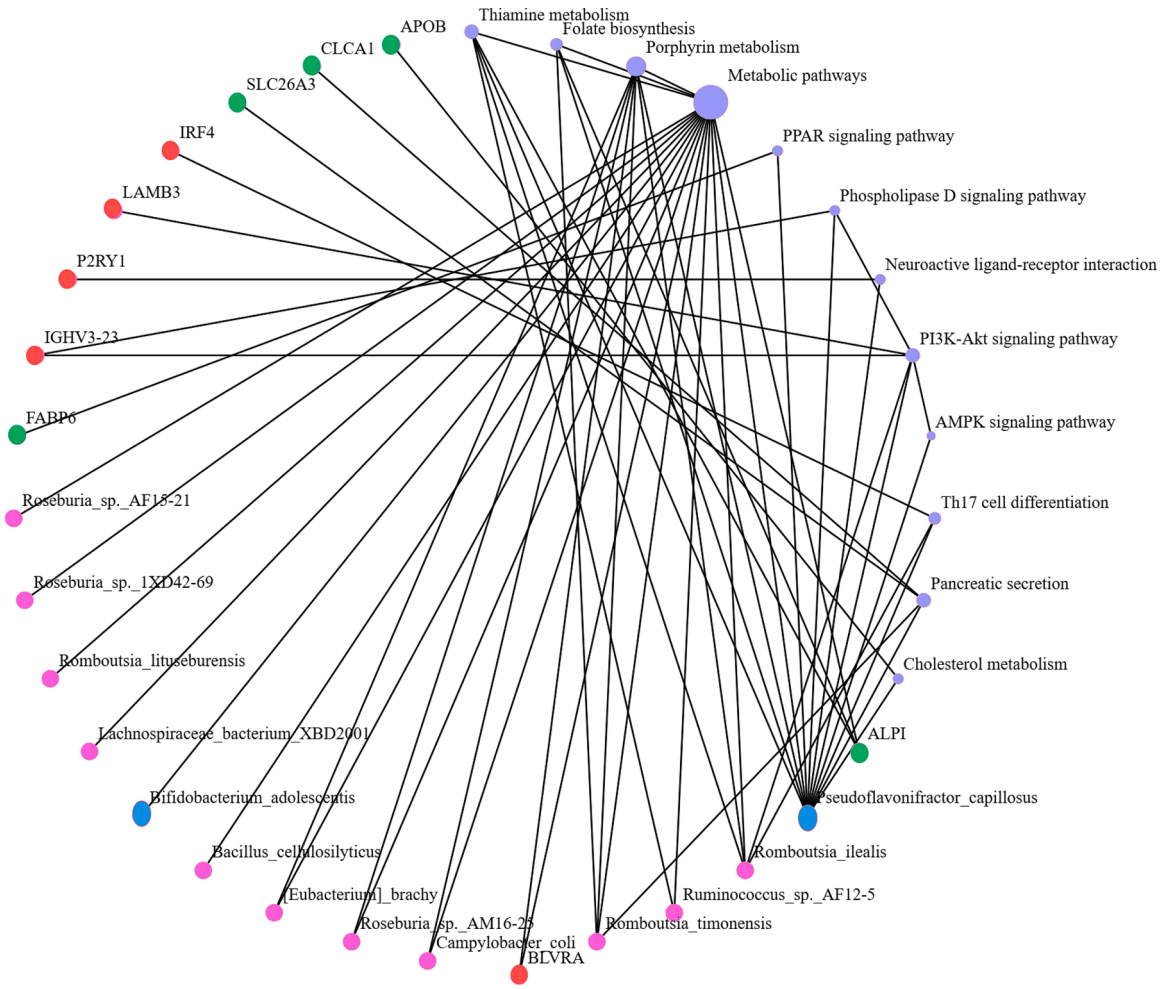

Fig. 14. Molecular network interaction analysis of genes associated with cecal tissue changes and microorganisms associated with cecal alterations in Liangshan Yanying chickens at different days of age.

Data availability

All raw data generated in this study have been deposited in the Genome Sequence Archive (GSA) at the National Genomics Data Center (NGDC), China National Center for Bioinformation/Beijing Institute of Genomics, Chinese Academy of Sciences (Genomics, Proteomics & Bioinformatics 2025; Nucleic Acids Res 2026), with the transcriptome data under accession number GSA: CRA044870 and the metagenomic sequencing data under accession number GSA: CRA044871. The data are publicly accessible at https://ngdc.cncb.ac.cn/gsa.

Funding

This study was funded by the PhD Research Launch Project of Xichang University"Research on molecular mechanism and genetic mechanism of chicken cecum flora specific colonization on biological function regulation (YBZ202211)"and the Liangshan Prefecture Science and Technology Program project "Investigation of Germplasm Resources and Research on Germplasm Innovation of Core Populations of Liangshan Primitive Chickens" (24YZGG0003).

CRediT authorship contribution statement

Zengwen Huang: Writing – review & editing, Writing – original draft, Funding acquisition. **Jing Wang:** Formal analysis, Data curation. **Chaoyun Yang:** Software, Investigation. **Zengpeng Lv:** Software, Formal analysis, Data curation. **Runjin Wang:** Resources, Methodology.

Disclosures

The authors declare that they have no competing interests.

Acknowledgement

The authors thank all animal breeders and farmers who provided the raw material for the experiments. The authors are also grateful to all the members of the research group for their contribution.

Supplementary materials

Supplementary material associated with this article can be found, in the online version, at doi:10.1016/j.psj.2026.106904.

References

Brisbin, J.T., Gong, J., Sharif, S., 2008. Interactions between commensal bacteria and the gut-associated immune system of the chicken. Anim. Health Res. Rev. 9, 101–110.

Cao, X. Y. 2011. Effects of dietary fiber levels on serum biochemical indices, production performance and digestive physiology of Gushi chickens.

Chen, L.Y., Li, S..F., Zhao, Z.H., 2014. Comparison of digestive organ development and feed utilization in different broiler lines and their hybrid progenies. Chin. J. Anim. Sci. 50, 61–64.

Fang, L.Y., Chen, F..F., Chen, X.L., Zhou, J.L., Liu, L.L., Yang, Y.J., Li, Q.Q., Guo, A.W., 2018. Effects of different rearing modes on production performance and intestinal and organ indices of broilers. China Poult 40, 31–34.

Gerritsen, J., Hornung, B., Renckens, B., van Hijum, S., Martins Dos Santos, V., Rijkers, G. T., Schaap, P.J., de Vos, W.M., Smidt, H., 2017. Genomic and functional analysis of *Romboutsia ilealis* CRIB(T) reveals adaptation to the small intestine. PeerJ. 5, e3698.

Guan, L.H., Liu, H..B., Zhang, L.Y., Wang, Z.W., Su, T.J., 2017. Effects of dietary energy levels on digestive organ development, relative content of muscle fatty acids and immune organ index of Saibei silky chickens. Henan Agric. Sci. 46, 106–109.
Huang, Z., Wang, J., Yang, C., Wang, R., 2026. Transcriptomic analysis of gene expression patterns in the Cecal tissue of Liangshan Yanying Chickens and Arbor Acres (AA) chickens before 28 days of age. Animals (Basel) 16, 474.
Hu, L. L. 2.013. Effects of enzyme preparations and energy levels on growth performance, digestive tract development and endogenous enzyme activities of broilers.
Kamada, N., Seo, S.U., Chen, G.Y., Núñez, G., 2013. Role of the gut microbiota in immunity and inflammatory disease. Nat. Rev. Immunol. 13, 321–335.
La Reau, A.J., Suen, G., 2018. The ruminococci: key symbionts of the gut ecosystem. J. Microbiol. 56, 199–208.
Latek, U., Chłopecka, M., Karlik, W., Mendel, M., 2022. Phytogenic compounds for enhancing intestinal barrier function in poultry-a review. Planta Med. 88, 218–236.
Perlot, T., Penninger, J.M., 2013. ACE2 - from the renin-angiotensin system to gut microbiota and malnutrition. Microb. Infect. 15, 866–873.
Rodrigues, D.R., 2022. Role of early life intestinal microbiota in modulating immunity in broiler chickens. Microbiomes Humans Animals Plants Environ. 225–242.
Rodríguez, J.M., Murphy, K.., Stanton, C., Ross, R.P., Kober, O.I., Juge, N., Avershina, E., Rudi, K., Narbad, A., Jenmalm, M.C., Marchesi, J.R., Collado, M.C., 2015. The composition of the gut microbiota throughout life, with an emphasis on early life. Microb. Ecol. Health Dis. 26, 26050.
Saad, A.H., Ahmed, M..S., Aboubakr, M., Ghoneim, H.A., Abdel-Daim, M.M., Albadrani, G.M., Arafat, N., Fadland, S.E., Abdo, W., 2021. Impact of dietary or drinking water *ruminococcus* sp. Supplementation and/or heat stress on growth, histopathology, and bursal gene expression of broilers. Front. Vet. Sci. 8, 663577.
Stanley, D., Hughes, R.J., Moore, R.J., 2014. Microbiota of the chicken gastrointestinal tract: influence on health, productivity and disease. Appl. Microbiol. Biotechnol. 98, 4301–4310.
Wang, M., Lkhagva, E., Kim, S., Zhai, C., Islam, M.M., Kim, H.J., Hong, S.T., 2024. The gut microbe pair of *oribacterium* sp. GMB0313 and *ruminococcus* sp. GMB0270 confers complete protection against SARS-CoV-2 infection by activating CD8+ T cell-mediated immunity. Gut. Microbes 16, 2342497.
Wickramasuriya, S.S., Park, I., Lee, K., Lee, Y., Kim, W.H., Nam, H., Lillehoj, H.S., 2022. Role of physiology, immunity, microbiota, and infectious diseases in the gut health of poultry. Vaccines (Basel) 10.
Xiao, Y., Xiang, Y., Zhou, W., Chen, J., Li, K., Yang, H., 2017. Microbial community mapping in intestinal tract of broiler chicken. Poult. Sci. 96, 1387–1393.
Yan, W., Sun, C., Yuan, J., Yang, N., 2017. Gut metagenomic analysis reveals prominent roles of *Lactobacillus* and cecal microbiota in chicken feed efficiency. Sci. Rep. 7, 45308.
Yeoman, C.J., Chia, N.., Jeraldo, P., Sipos, M., Goldenfeld, N.D., White, B.A., 2012. The microbiome of the chicken gastrointestinal tract. Anim. Health Res. Rev. 13, 89–99.
Yin, H., Huang, J., Guo, X., Xia, J., Hu, M., 2023. *Romboutsia lituseburensis* JCM1404 supplementation ameliorated endothelial function via gut microbiota modulation and lipid metabolisms alterations in obese rats. FEMS Microbiol. Lett. 370, fnad016.
Young, J.C., Zhou, T., Yu, H., Zhu, H., Gong, J., 2007. Degradation of trichothecene mycotoxins by chicken intestinal microbes. Food Chem. Toxicol. 45, 136–143.
Zhang, Y. 2019. Community structure and functional genes of chicken intestinal microbiota and healthy breeding of chickens.
Zhu, X.Y., Zhong, T., Pandya, Y., Joerger, R.D., 2002. 16S rRNA-based analysis of microbiota from the cecum of broiler chickens. Appl. Environ. Microbiol. 68, 124–137.